Optical Materials 72 (2017) 177–182

Contents lists available at ScienceDirect

Optical Materials

journal homepage: www.elsevier.com/locate/optmat

Quantum and conversion efficiencies optimization of superstrate CIGS thin-films solar cells using In_2Se_3 buffer layer

Idris Bouchama [a], Samah Boudour [a, b, c], Nadir Bouarissa [d, *], Zahir Rouabah [e]

[a] Electronic Department, Faculty of Technology, University M. Boudiaf, 28000, Msila, Algeria
[b] Research Centre in Industrial Technologies CRTI, P.O. Box 64, Cheraga, 16014, Algiers, Algeria
[c] Thin Films and Applications Unit (UDCMA), Setif, Algeria
[d] Laboratory of Materials Physics and its Applications, University of M'sila, 28000, M'sila, Algeria
[e] Materials and Electronic Systems Laboratory, University of Bordj-Bou-Arreridj, 34000, Bord-Bou-Arreridj, Algeria

ARTICLE INFO

Article history:
Received 27 March 2017
Received in revised form
26 May 2017
Accepted 30 May 2017

Keywords:
$Cu(In,Ga)Se_2$ material
Superstrate solar cells
Transparent conducting oxides
Barrier height
AMPS-1D

ABSTRACT

In this present contribution, AMPS-1D device simulator is employed to study the performances of superstrate SLG/TCO/p-$Cu(In,Ga)Se_2$(CIGS)/n-ODC/n-In_2Se_3/Metal thin film solar cells. The impact of the TCO and Metal work functions on the cell performance has been investigated. The combination of optical transparency and electrical property for TCO front contact layer is found to yield high efficiency. The obtained results show that the TCO work function should be large enough to achieve high conversion efficiency for superstrate CIGS solar cell. Nevertheless, it is desirable for Metal back contact layer to have low work function to prevent the effect of band bending in the n-In_2Se_3/Metal interface. Several TCOs materials and metals have been tested respectively as a front and back contact layers for superstrate CIGS solar cells. An efficiency of 20.18%, with $V_{oc} \approx 0.71$ V, $J_{sc} \approx 35.36$ mA/cm^2 and $FF \approx 80.42\%$, has been achieved with $ZnSn_2O_3$-based as TCO front contact layer. In the case of SnO_2:F front contact and indium back contact layers, an efficiency of 16.31%, with $V_{oc} \approx 0.64$ V, $J_{sc} \approx 31.4$ mA/cm^2 and $FF \approx 79.4\%$, has been obtained. The present results of simulation suggest an improvement of superstrate CIGS solar cells efficiency for feasible fabrication.

1. Introduction

$CuIn_{1-x}Ga_xSe_2$ (CIGS) has a major potential as a semiconductor material for thin film photovoltaic devices. This is due to its high optical absorption coefficient, appropriate band gap and outstanding electro-optical properties [1–3]. CIGS-based solar cells with x = 0.3 corresponds to a bandgap energy range of 1.1–1.2 eV yields the best efficiency both in laboratory and commercial solar cells [4,5]. Recently CIGS thin film solar cells approached efficiencies of 22.8% for substrate configuration [6]. The superstrate configuration is an alternate design, where the deposition sequence is reversed, the absorber is grown on glass coated with the transparent front contact (TFC), followed by an evaporated CdS or In_2Se_3 buffer layers and finished by a sputtered metallic back contact layer [7–9]. Further improvements of the superstrate CIGS solar cells performance require an accurate knowledge of the electronic loss mechanisms.

The properties of Transparent conducting oxide (TCO) films, such as resistivity, band-gap energy and work function, affect obviously the performance of solar device because they affect both the energy barrier height at the heterojunction interfaces and the electron field emission [10]. TCO films are n-type degenerated semiconductors (metallic oxides), they are formed from binary oxides, such as In_2O_3, SnO_2 and ZnO; ternary oxides, such as $Zn_2In_2O_5$, Zn_2SnO_4, $CdSb_2O_6$, $MgIn_2O_4$, $ZnSnO_3$, $GaInO_3$, and $In_4Sn_3O_{12}$ and multi-component oxides composed of combinations of these binary or ternary oxides [11]. The work function of the TCO films (W_{TCO}) has a critical importance in optoelectronic device performance, the change in work function and electron/hole injection barrier is related to the band alignment [12–14]. Ritzau et al. [15] have reported the role of the work function and back contact barrier height on the performance of a-Si:H solar cells. Besides, Belfar et al. [16] investigated the effect of W_{TCO} for the performance of n–i–p+ and n–i–p–p+ solar cells based on hydrogenated amorphous silicon (a-Si:H) and hydrogenated nanocrystalline silicon (nc-Si:H) absorber layers using AMPS-1D simulation tools. Furthermore, Hussain et al. [17] reported

* Corresponding author.
E-mail address: n_bouarissa@yahoo.fr (N. Bouarissa).

http://dx.doi.org/10.1016/j.optmat.2017.05.056
0925-3467/

that the high work function of ITO films can be used for barrier height modification of HIT solar cell and the wide band gap and highly doped ITO films behave electronically similar to metals elements and the electronic behavior of the ITO/*a*-Si:H(p) interface was assumed as similar to a metal/semiconductor junction. Recently, Bouchama et al. [18] have reported that the CIGS solar cell with superstrate configuration has a better photovoltaic performances when lighting through SnO_2:F front contact layer. Moreover, an efficiency higher than 16%, could be obtained for superstrate SLG/SnO_2:F/CIGS/ODC/In_2Se_3/Zn solar cell structure for 300 nm p-CIGS absorber thick.

This paper reports on systematic studies of TCO and Metal work functions including a discussion of their dependence on the superstrate SLG/TCO/p-CIGS/n-ODC/n-In_2Se_3/Metal solar cells photovoltaic properties. Our study is focused on reducing the potential barriers so as to increase carriers collection in the structure.

2. Device simulation and modeling

The model used in the simulation is simple as shown in Fig. 1. Up to five regions of different material parameters can be used to define the cell structure. The structure consists of SLG/TCO/p-$CuIn_{0.7}Ga_{0.3}Se_2$/n-ODC/n-In_2Se_3/Metal in which the light enters through the TCO layer is considered as the solar cell model in the simulation. We insert in the model a significant Ordered Defect Compounds (ODC) n-type layer between the In_2Se_3 and CIGS layers. This layer is usually created experimentally in the CIGS absorber part when the In_2Se_3 buffer layer is deposited onto SLG/TCO/CIGS substrate with high substrate temperature [8,9]. The AMPS-1D software estimates the steady state band diagram, recombination profile, carrier transport in one dimension based on the Poisson equation and the hole and electron continuity equations [19]. The recombination currents are calculated with the Shockley–Read–Hall (SRH) model

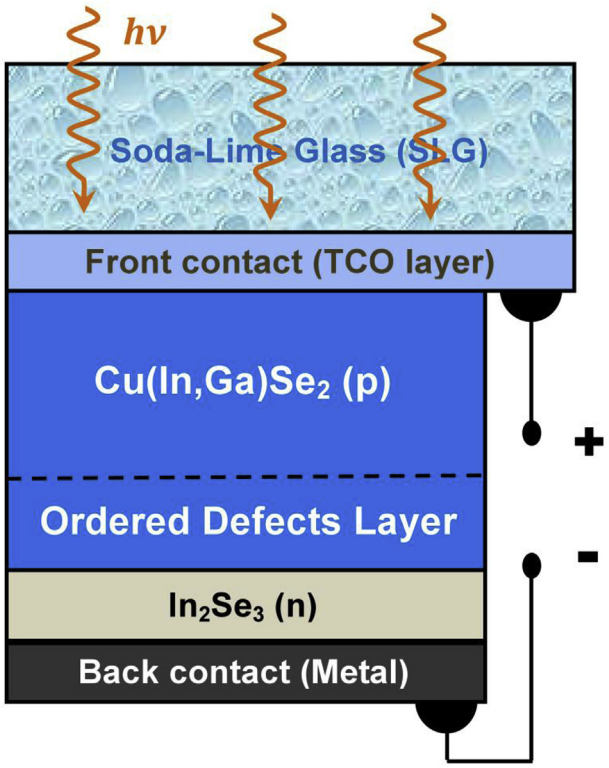

Fig. 1. Schematic cross section of superstrate CIGS solar cell structure.

for bulk defects. The layers parameters used for simulating the device performance are summarized in Table 1. The $CuIn_{0.7}Ga_{0.3}Se_2$ absorber and In_2Se_3 buffer parameters were fixed from our previous research work [18]. The radiation AM1.5G with incident power density of 100 mW/cm^2 is used as an illuminating source. In superstrate CIGS solar cells, a highly doped TCO front contact and Metal back contact layers serve as the front and back electrodes, respectively.

3. Results and discussion

3.1. Effect of TCO work function on cell performance

In the superstrate CIGS structure presented in Fig. 1, an n+-type TCO front contact can be believed to form a barrier with p-CIGS absorber part. The formation of a low resistance, low barrier TCO/p-CIGS front contact is among the most challenging aspects of high performance fabrication of superstrate CIGS solar cells. The wide band gap and highly doped TCO films behave electronically similar to metals elements and the electronic behavior of the TCO/semiconductor interface was assumed as similar to a metal/semiconductor junction [17]. Moreover, the TCO/p-type CIGS contact does not always form a barrier and has the possibility of forming an ohmic contact, which is determined by the difference in work functions between TCO and p-CIGS [20]. For a p-CIGS type semiconductor with band-gap E_g and electron affinity χ(CIGS), and a TCO with work function W_{TCO}, an ohmic TCO/p-CIGS contact is formed when: $W_{TCO} > E_g + \chi$(CIGS) and a rectifying (Schottky) barrier contact is formed when $W_{TCO} < E_g + \chi$(CIGS) [21]. Most TCO materials, however, do not have sufficiently high work-functions and therefore form a Schottky barrier contact to p-CIGS absorber layer.

The understanding of the effects of TCO work function on TCO/p-CIGS/n-ODC/n-In_2Se_3 solar cells in depth requires the calculation of the energy band diagram at thermodynamic equilibrium and the built-in electric field. Fig. 2 depicts the schematic band diagram of the TCO/p-CIGS/ODC part for different TCO work functions. The band bending on the p-CIGS part appeared along with the decrease of TCO work function. Two possible carrier transport mechanisms were expected. In the case of high TCO work function, an ohmic contact was formed in n+-TCO/p-CIGS interface and a direct recombination of holes in the valence band of p-CIGS and electrons in the conduction band of n+-TCO was occurred. The second is a trap-assisted tunneling even if the barrier is formed at the n+-TCO/p-CIGS interface [20]. Photogenerated holes in p-CIGS part can passes across the Schottky barrier and reach TCO contact easily thanks to a trap-assisted tunneling.

Table 1
Physical parameters used in the simulation model for superstrate CIGS solar cell.

Layer parameters	p–CIGS	n–ODC	n–In_2Se_3
W (nm)	500	3500	200
N_D (cm^{-3})	–	1×10^{15}	1×10^{18}
N_A (cm^{-3})	2×10^{16}	–	–
E_G (eV)	1.12	1.3	2.4
χ (eV)	4.1	4.1	3.8
N_c (cm^{-3})	2.2×10^{18}	2.2×10^{18}	2.2×10^{18}
N_v (cm^{-3})	1.8×10^{19}	1.8×10^{19}	1.8×10^{19}
$\varepsilon/\varepsilon_0$ (–)	13.6	13.6	10
μ_e (cm^2 V^{-1} S^{-1})	50	50	50
μ_h (cm^2 V^{-1} S^{-1})	12	12	12
N_{DG}, N_{AG} (cm^{-3})	D: 10^{14}	A: 10^{18}	A: 10^{18}
E_A, E_D (eV)	Mid–gap	Mid–gap	Mid–gap
W_G (eV)	0.1	0.1	0.1
σ_e (cm^2)	10^{-13}	10^{-13}	10^{-15}
σ_h (cm^2)	10^{-15}	10^{-11}	10^{-12}

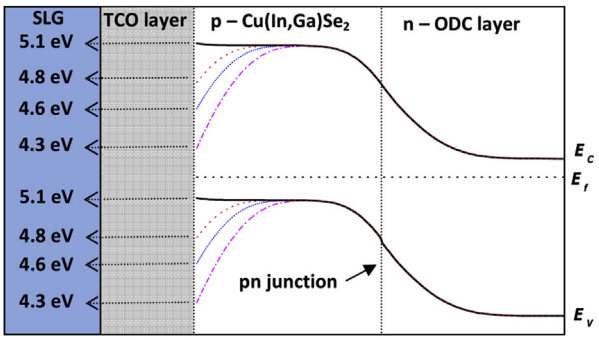

Fig. 2. Band structure in the TCO/p-CIGS interface with different TCO work functions.

The performance of superstrate SLG/TCO/p-CIGS/ODC/n-In_2Se_3/Metal solar cells will be investigated numerically by the variation of TCO work function (W_{TCO}). In the model, P-type CIGS and ODC layer parameters were fixed, and only the work function of TCO films was changed from 4 to 5.5 eV. Zn material was used in this section as a back contact. When TCO work function is below 5 eV, the transport of holes is limited because of the occurrence of the band bending in the p-CIGS part. In the case of the TCO work function is higher than 5 eV, the band bending in the p-CIGS absorber part is reduced to form a flat band. The increase in W_{TCO} leads to the decrease of the Schottky barrier height between TCO and p-CIGS layer; therefore more hole carriers can be collected at the front contact.

Different TCO work functions at the interface between TCO and p-CIGS layer will lead to different built-in electric field. Fig. 3 shows the distribution of built-in electric field in the structure as a function of TCO work function. Note that the electric field decreases gradually in the p-CIGS part near the TCO/p-CIGS interface. Nevertheless, in the region of n-ODC layer the built-in electric field keeps unchanged. In the p-CIGS part with $W_{TCO} \leq 5$ eV, the built-in electric field is positive near the interface, which hinders holes from reaching the front electrodes. When $W_{TCO} > 5.1$ eV, the built-in electric field is negative in the whole of p-CIGS region. This electric field gives the effective force on holes to move to the left region in Fig. 3, which is very beneficial for holes to transport through the p-CIGS region.

One of the aims of this simulation is to determine the proper work function of TCO front contact for designing high conversion efficiency of superstrate CIGS solar cell. So, it is necessary to calculate the photovoltaic parameters of the solar cell on the wide range

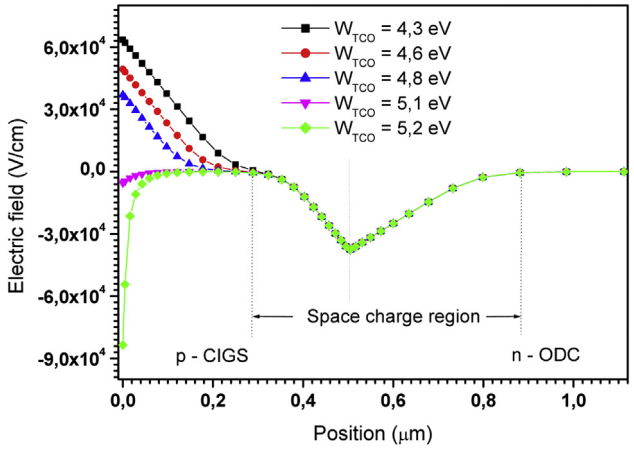

Fig. 3. Distribution of built-in electric field in the structure with various TCO work functions.

of variation of W_{TCO}. Fig. 4 shows the simulated performance of SLG/TCO/p-CIGS/n-ODC/n-In_2Se_3/Metal solar cells as a function of TCO work function. It is easy to note that when W_{TCO} is varied between 4.3 eV and 5.0 eV, the TCO work function has a little impact on J_{SC}. The open-circuit V_{OC} increases rapidly with W_{TCO}, and then become saturated at $W_{TCO} = 4.8$ eV. As the W_{TCO} increases, *FF* also increases due to the migration of holes from p-CIGS part to TCO front contact since the hole injection barrier was reduced. Reduction of the band bending was due to the decrease of the electric field at TCO/p-CIGS interface which can provide low leakage current. At $W_{TCO} = 4.8$ eV, we can achieve an efficiency of about 15.02%, $FF = 80.06\%$, $V_{OC} = 0.63$ V, $J_{SC} = 29.23$ mA/cm^2. It is obvious that at $W_{TCO} = 4.3$ eV, the cell has a poor performance with $\eta = 2.08\%$, $FF = 51.4\%$, $V_{OC} = 0.13$ V and $J_{SC} = 29.21$ mA/cm^2, while at $W_{TCO} = 5.4$ eV, the cell has a good performance with $\eta = 20.71\%$, $FF = 81.80\%$, $V_{OC} = 0.71$ V and $J_{SC} = 35.32$ mA/cm^2. The structure with TCO work function below 4.2 eV does not work at all. This simulation result manifests the critical effect of TCO work function in superstrate CIGS solar cells.

The front contact processes are designed to reduce the downward band-bending in the TCO/p-CIGS interface so that the barrier to holes is reduced and current can be collected. Several TCO layers have been tested in the model as a front contact layers for superstrate CIGS solar cells. Fig. 5 shows the cell-performance results with different TCO front contact layers. $ZnSnO_3$ n-type semiconductor with the wide band gap and high work function of ~5.3 eV, considered as a front contact material, is a potential

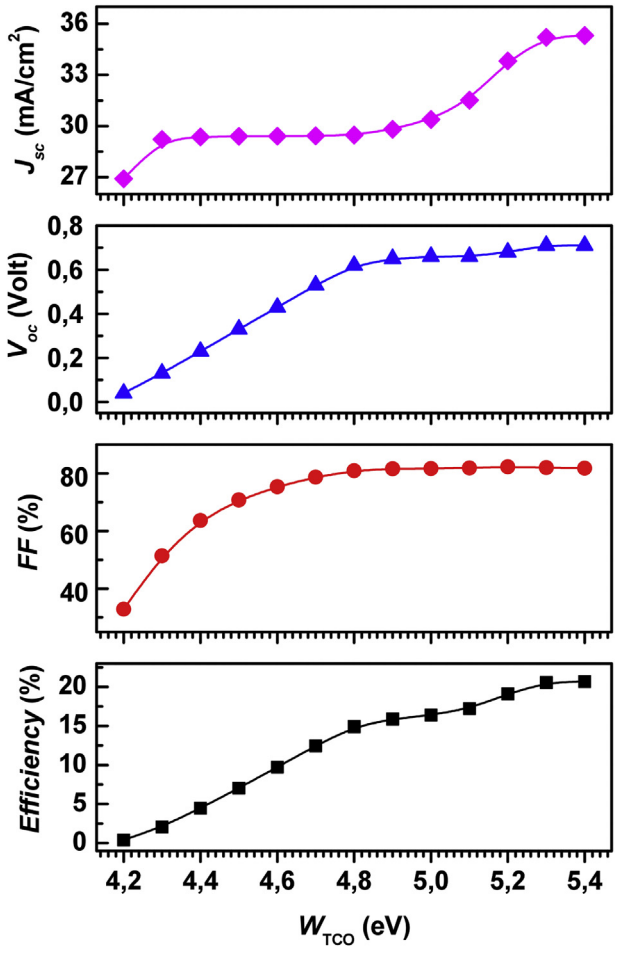

Fig. 4. Performance of superstrate CIGS solar cells as a function of TCO work function.

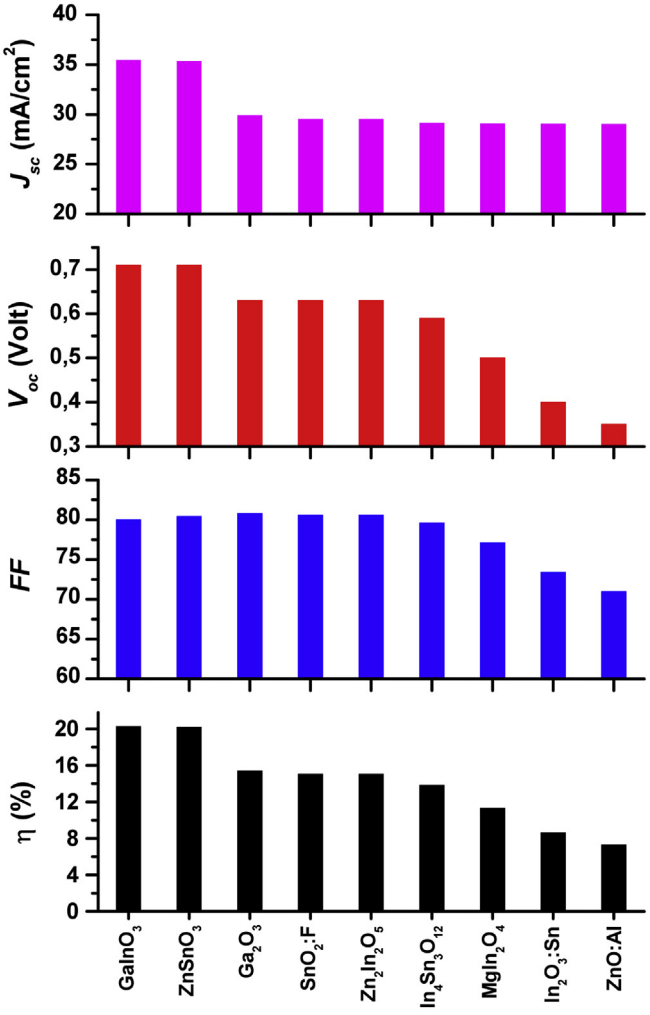

Fig. 5. A summary results of superstrate CIGS solar cells performances with different TCO films.

candidate for a good TCO. With $ZnSnO_3$ front contact we can achieve an efficiency of 20.17%, with $V_{oc} \approx 0.71$ V, $J_{sc} \approx 35.35$ mA/cm^2 and $FF \approx 80.4\%$. ITO films have a low work function which is about 4.6 eV. This degrades the conversion efficiency of solar cells to 8.63%. Solar cell with ZnO:Al front contacts showed also a poor efficiency of 7.31%. The SnO_2:F material with a work function of ~4.9 eV is another candidate similarly to TCO front contact for superstrate CIGS solar cells presenting an efficiency of 15.06%.

Spectral response of various TCO work functions was studied and presented in Fig. 6. With increasing W_{TCO}, the spectral response increases in short wavelength region. The quantum efficiency (QE) has a maximum value close to 80% under 100 mW/cm^2 when the TCO work function reaches 5.2 eV.

3.2. Effect of back metal work function

The metal back contact forms a barrier to n-type In_2Se_3 semiconductor which depends on the work function of both Metal and n-In_2Se_3 material. If the work function of an n-type In_2Se_3 semiconductor ($W_{n\text{-}SC}$) is greater than that of the Metal (W_{Metal}), $W_{n\text{-}SC} > W_{Metal}$, then the n-$In_2Se_3$/Metal heterojunction forms an ohmic contact. If the relative magnitudes are reversed, i.e. $W_{n\text{-}SC} < W_{Metal}$, then the n-$In_2Se_3$/Metal heterojunction forms a blocking or Schottky barrier [22]. The band bending in the n-In_2Se_3 buffer layer

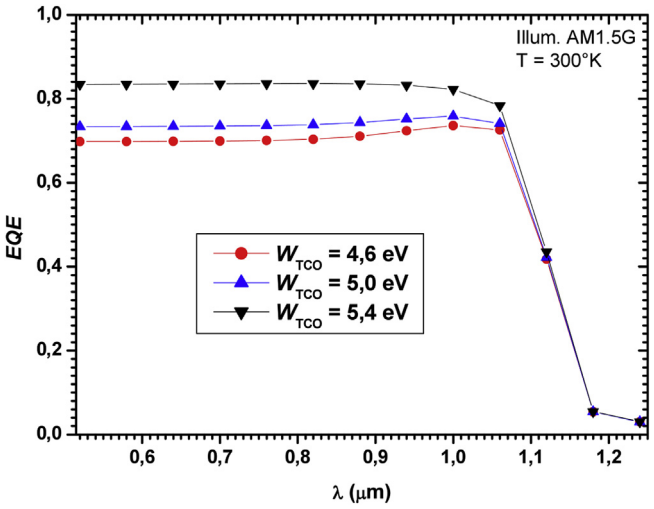

Fig. 6. Effect of TCO work function on the spectral response.

was occurs in the vicinity of the interface. The carrier (electron) transport across n-In_2Se_3/Metal interface is greatly affected by the barrier height resulting in the n-In_2Se_3/Metal interface. At high Metal work function, the tunneling mechanism through the barrier dominates the current transport with high doping n-type In_2Se_3 semiconductor used in the simulation ($N_D(In_2Se_3) = 1 \times 10^{18}$ cm^{-3}), while the thermionic emission acts as a secondary transport mechanism in the n-In_2Se_3/Metal interface. In the case of the thermal emission, the electron has to overcome the whole energy barrier, however, the tunneling takes place through the energy spike resulting in the n-In_2Se_3/Metal interface. The barrier height Φ_b is defined as the potential difference between the Fermi energy of the metal and the band edge where the majority carrier reside. For n-type In_2Se_3 semiconductor the barrier height is obtained as [23]:

$$\Phi_b = W_{Metal} - \chi(In_2Se_3) \quad (1)$$

where W_{Metal} is the work function of the metal and $\chi(In_2Se_3)$ is the electron affinity of the n-In_2Se_3 semiconductor. Fig. 7 shows the work function of selected metals and their calculated barrier height on n-In_2Se_3 part, where the metal work functions varied between 4.1 and 5.2 eV. We can see that the barrier height in the n-In_2Se_3/Metal interface can be varied from 0.2 to 1.3 eV by using various

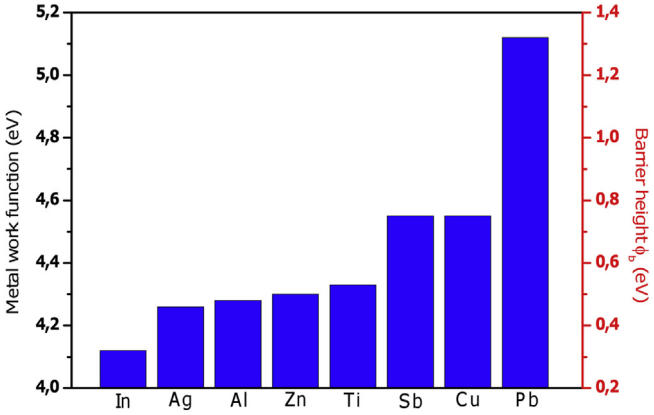

Fig. 7. Work function of selected metals and their calculated barrier height on n-type In_2Se_3 buffer layer.

metals.

To find the influence of the barrier height Φ_b, on cell performance, we have firstly varied the value of Φ_b from 0.46 to 0.6 eV and the simulated current density-voltage (J-V) characteristics are shown in Fig. 8. The results of the calculation were obtained by using SnO_2:F as a TCO front contact layer. It is evident from the behavior of the curves that only the fill factor *FF* was degraded with increasing the barrier height Φ_b. This may be due to the increase in the resistance and the presence of the rectifying n-In_2Se_3/metal junction which forms a Schottky barrier in the structure (Fig. 8). The high potential barrier prevents most charge carriers (electrons) from passing to the metal back contact. Only a small number of carriers have enough energy to overcome the whole energy barrier (thermoionic emission), however, the tunneling effect takes place in some cases. To clarify this dependence in an interval of variation, the barrier height Φ_b was varied from 0 to 0.9 eV.

Fig. 9 summarizes the output performance of J_{SC}, V_{OC}, fill factor (*FF*) and η as a function barrier height Φ_b. All photovoltaic parameters remain almost constant for barrier height below 0.4 eV. By an increase in Φ_b of more than 0.4 eV an incredible decrease in efficiency, V_{OC} and *FF* was found as revealed from Fig. 9. In this case, the majority carriers have insufficient energy to overcome the potential barrier, and are trapped on back side of the interface and cannot contribute to the diffusion current, reducing thus the solar cell performance. It is evident from Fig. 9 that the short-circuit current J_{SC} has a slight decrease as the Φ_b increases from 0.4 to 0.9 eV, which may be due to the tunneling enhancement. The use of SnO_2:F front contact and Zn back contact layers in the structure reported in Ref. [18] led to an efficiency of 15.12%, with $V_{oc} \approx 0.63$ V, $J_{sc} \approx 31.4$ mA/cm^2 and $FF \approx 74.6\%$. Using low metal work function as a metal back contact, such as indium (4.12 eV), a best efficiency of 16.31%, with $V_{oc} \approx 0.64$ V, $J_{sc} \approx 31.4$ mA/cm^2 and $FF \approx 79.4\%$, has been obtained.

4. Conclusion

The presence of the barrier height in the front and back contact layers of the superstrate SLG/TCO/p-CIGS/n-ODC/n-In_2Se_3/Metal solar cells can significantly affect the cell performance by limiting the carriers current flow. The influence of the TCO and Metal work function has been studied using AMPS-1D and the corresponding design optimization has been provided. According to the obtained results, the TCO work function should be large enough of over 4.8 eV to prevent the effect of absorber band bending caused by the difference in the work function between the p-type CIGS absorber and TCO front contact. We notice that all the photovoltaic parameters increase with increasing the TCO work function. This remarkably sharp rise has also been confirmed by the external quantum efficiency. The high W_{TCO} is used to inject holes in the front contact barrier. Thus, the desired values of work functions should be as high as possible. The high work function of $ZnSnO_3$ material is helpful in making low-resistance electrical contact to the *p*-type CIGS layer. Secondly, a significant performance improvement of the cell efficiency can be expected through the minimization of barrier height ($\leq$0.45 eV) in the n-In_2Se_3/Metal interface. When the barrier height of the n-In_2Se_3/Metal interface exceeds 0.5 eV, the degradation came from the reduction of the fill-factor *FF* and open-circuit voltage V_{OC}. The present results may help in the development of superstrate CIGS solar cells with high conversion efficiency and low cost.

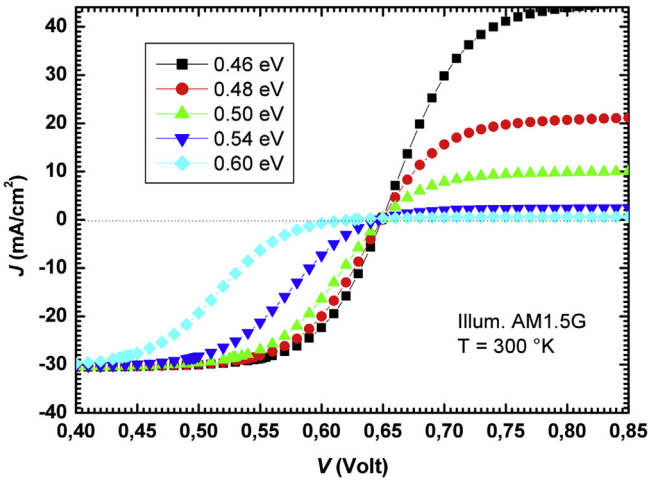

Fig. 8. J-V characteristics of the selected structure with different barrier heights Φ_b.

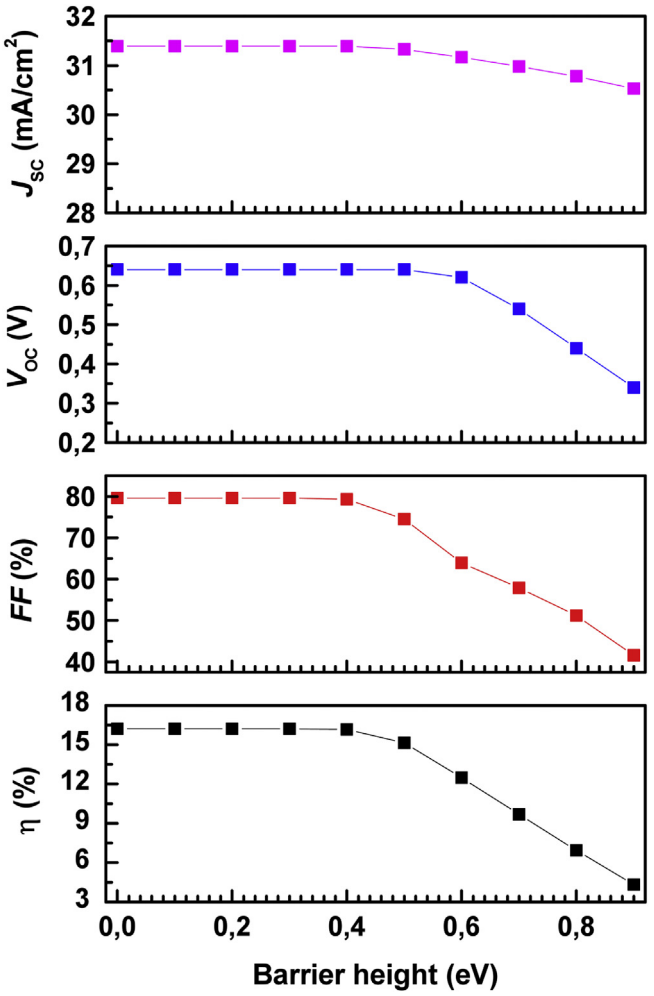

Fig. 9. Solar cell performances as a function of barrier height at the n-In_2Se_3/Metal interface.

Acknowledgements

The modeling calculation of this work used the AMPS-1D software developed by Dr. Fonash's group of Pennsylvania State University.

References

[1] J. Lauwaert, L.V. Puyvelde, J. Lauwaert, J.W. Thybaut, S. Khelifi, M. Burgelman,

F. Pianezzi, A.N. Tiwari, H. Vrielinck, Assignment of capacitance spectroscopy signals of CIGS solar cells to effects of non-ohmic contacts, Sol. Energy Mater. Sol. Cells 112 (2013) 78–83.
[2] S.U. Park, R. Sharma, K. Ashok, S. Kang, J.K. Sim, C.R. Lee, A study on composition, structure and optical properties of copper-poor CIGS thin film deposited by sequential sputtering of CuGa/In and In/(CuGa+In) precursors, J. Cryst. Growth 359 (2012) 1–10.
[3] A. Bouloufa, K. Djessas, D. Todorovic, Mat. Sci. Semicond. Proc. 12 (2009) 82.
[4] T. Eisenbarth, T. Unold, R. Caballero, C.A. Kaufmann, D. Abou-Ras, H.-W. Schock, Origin of defects in $CuIn_{1-x}Ga_xSe_2$ solar cells with varied Ga content, Thin Solid Films 517 (2009) 2244–2247.
[5] R. Baier, C. Leendertz, D. Abou-Ras, M.C. Lux-Steiner, S. Sadewasser, Sol. Energy Mater. Sol. Cells 130 (2014) 124–131.
[6] R. Kamada, T. Yagioka, S. Adachi, A. Handa, K. FaiTai, T. Kato, H. Sugimoto, New world record $Cu(In,Ga)(Se,S)_2$ thin film solar cell efficiency beyond 22%, in: 43rd IEEE Photovoltaic Specialists Conference, #355, 2016 available at: http://www.pvsc-proceedings.org/.
[7] K. Djessas, A. Abatchou, G. Masse, J. Appl. Phys. 88 (2000) 5710.
[8] K. Djessas, S. Yapi, G. Masse, J. Appl. Phys. 95 (2004) 4111.
[9] G. Masse, K. Djessas, J. Appl. Phys. 94 (2003) 6985.
[10] T. Minami, J. Vac. Sci. Technol. A 17 (1999) 1765–1772.
[11] T. Minami, T. Miyata, T. Yamamoto, Work function of transparent conducting multicomponent oxide thin films prepared by magnetron sputtering, Surf. Coat. Tech. 108–109 (1998) 583–587.
[12] L. Zhao, C.L. Zhou, H.L. Li, H.W. Diao, W.J. Wang, Sol. Energy Mater. Sol. Cells 92 (2008) 673–681.
[13] T. Minemoto, J. Julayhi, Curr. Appl. Phys. 13 (2013) 103–106.
[14] A. Chen, K. Zhu, Sol. Energy 107 (2014) 195–201.
[15] K.U. Ritzau, M. Bivour, S. Schröer, H. Steinkemper, P. Reinecke, F. Wagner, M. Hermle, TCO work function related transport losses at the a-Si:H/TCO-contact in SHJ solar cells, Sol. Energy Mater. Sol. Cells 131 (2014) 9–13.
[16] A. Belfar, Simulation study of the a-Si:H/nc-Si:H solar cells performance sensitivity to the TCO work function, the band gap and the thickness of i-a-Si:H absorber layer, Sol. Energy 114 (2015) 408–417.
[17] S.Q. Hussain, W.K. Oh, S. Ahn, A.H.T. Le, S. Kima, Y. Lee, J. Yi, RF magnetron sputtered indium tin oxide films with high transmittance and work function for a-Si:H/c-Si heterojunction solar cells, Vacuum 101 (2014) 18–21.
[18] I. Bouchama, K. Djessas, F. Djahli, A. Bouloufa, Thin Solid Films 519 (2011) 7280–7283.
[19] H. Zhu, A.K. Kalkan, J. Hou, S.J. Fonash, AIP Conf. Proc. 462 (1999) 309.
[20] T. Nakada, Y. Hirabayashi, T. Tokado, D. Ohmori, T. Mise, Sol. Energy 77 (2004) 739–747.
[21] S.H. Demtsu, Impact of Back-contact Materials on Performance and Stability of CdS/CdTe Solar Cells, PhD Thesis, Colorado State University, Fort Collins, Colorado, 2006.
[22] W. Mönch, Semiconductor Surfaces and Interfaces, Third Revised Edition, Springer, 2001.
[23] L. Zhu, G. Shao, J.K. Luo, Numerical study of metal oxide Schottky type solar cells, Solid State Sci. 14 (2012) 857–863.